Application Note
Gear-Tooth Detection With Back-Biased 3D Hall-Effect Sensors

<div style="text-align:right">**TEXAS INSTRUMENTS**</div>

Scott Bryson

ABSTRACT

Vehicle sensing systems including e-bike cadence detection and anti-lock brake systems function by measuring the speed and direction a rotating pedal crankset or wheel. Mechanical designs wear over time, and optical sensors can be cumbersome and difficult to keep free of dirt and debris.

An alternative approach using a fixed position back-biased Hall-effect sensor can provide a high degree of resolution to provide not only the speed of rotation, but the direction and relative angle measurements to detect small changes to the system as well. Back-biased sensors operate by measuring the interaction of a magnetic field and a moving ferromagnetic object.

Table of Contents

Trademarks
All trademarks are the property of their respective owners.

1 Introduction

Many critical functions in automotive vehicle systems including anti-lock braking systems (ABS), odometer, speedometer, and traction control rely on measuring the rotation speed of each wheel. Similarly in e-bikes this function is necessary not only to measure the traveling speed of the bicycle, but it is necessary to monitor the speed of rotation in the pedal crankset. This data is not only useful for fitness training computers that calculate a rider's energy output, but the data also provides confirmation that the rider is actively pedaling. This signal is required before the microcontroller enables motor output and is also used to set the motor speed based on programmed rider assist settings.

In many cadence monitor systems, this function has been implemented by placing a disc with several embedded magnets onto the pedal crankset. An example using 12 magnets is shown in Figure 1-1. With the magnets installed with alternating polarity, a 2D magnetic latch such as TMAG5110 can be used to track the passage of each magnet and provide a series of pulses as the magnet rotates.
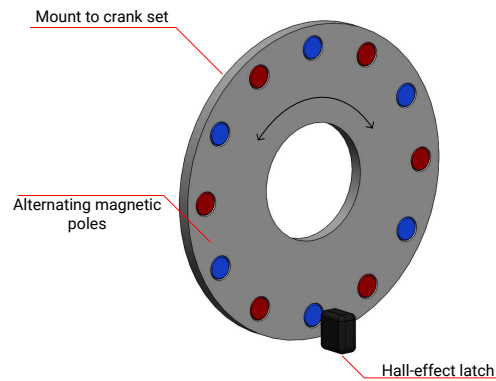
Figure 1-1. Discrete Magnet Cadence Monitor

When configured with a 2D latch, each pair of magnets can potentially create up to 4 transition states, for 24 total states per revolution in the pictured example. Alternatively, a single 1D latch can detect only 12 states - One for each magnet pole. If designed to achieve a 50% duty cycle, each state can represent about 15deg of rotation. While this is a relatively small amount of rotation, this can be challenging for the rider in cases where a heavier bike is stopped facing uphill. Additionally, the cost of the magnets and installation difficulty make this design less desirable.

Another possibility when using a bottom bracket mounted motor is to move the cadence detection interior to the motor. In these assemblies the pedals are connected to the motor output through a clutch. The clutch is disengaged until the rider pedals forward, and this protects the rider from injury that can occur by forcing the pedals to spin with the motor. In this system, it is possible to move the cadence sensor interior to the motor assembly using optical sensors. Even in this case, however, there is still potential for dirt and grease from the motor operation to contaminate the sensor over time.

Whether designed into the system, or connected as an external module, back-biased magnetic sensors can be used to provide this function with greater resolution than the traditional design and free from concern caused by optical contaminants. In a back-biased configuration, the magnet remains fixed in a stationary position relative to the magnetic sensor as shown in Figure 1-2.
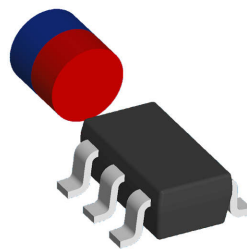
Figure 1-2. Back-Bias Configuration

The resulting field from the permanent magnet is then free to interact with the surroundings. When placed near a ferromagnetic gear or reluctance plate, the field from the stationary magnet can be drawn into the teeth of the gear. Since the range to the magnet changes as each tip and root of the gear teeth pass by, the strength of the magnetic flux density at the sensor can oscillate along multiple axes. Such an interaction is shown in the simulated field behavior depicted in Figure 1-3. Here, the field is distorted towards the nearby sprocket tooth to the right of the magnet.
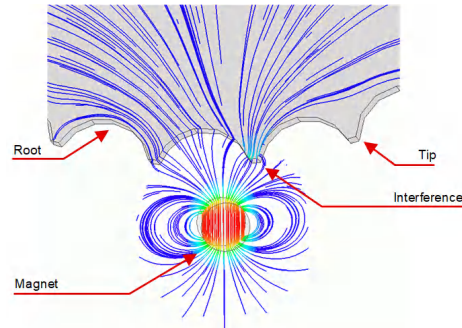
Figure 1-3. Magnetic Field Interaction

2 Implementation and Testing

2.1 Build Configuration

To demonstrate this behavior, a 32-tooth crankset and bottom bracket were mounted into a 3D printed assembly.

Figure 2-1. Gear Tooth Sensing Setup

A bracket to mount either the TMAG3001 (a small commercial grade 3D sensor in a WCSP package) or TMAG5173-Q1 (an automotive grade 3D sensor in a small SOT-23 package) with a back bias magnet was designed to position the sensor in near proximity to the rotating front sprocket. On this demonstration there is no chain, but in a practical setting this needs to be installed on the section of the sprocket where the chain does not rest.
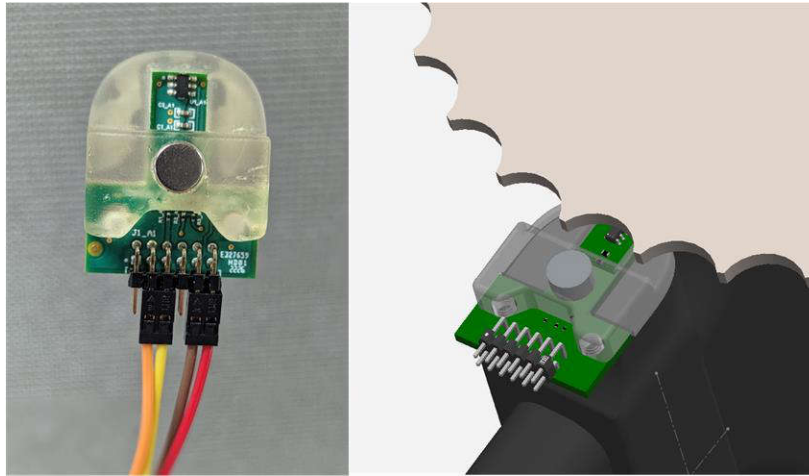
Figure 2-2. TMAG5173-Q1 Sensor and Back-bias Magnet Placement

For most riders, a pedal speed of 80-100 RPM is considered a designed for target when riding unassisted. Speeds above 110 RPM are typically only achieved during sprints. Suppose a target maximum speed of 150 RPM is set using a 32 tooth gear. In this case, the transit time for each tooth has a time span of approximately 78ms. In this case, we can calculate a desired sample rate based on the number samples per tooth.

While the Nyquist rate can require only 2 samples per oscillation as a minimum to detect each tooth, it is typically desirable to sample at a higher rate to gather a more complete profile. Consider below what is observed for the Nyquist rate compared to sampling 5 times per oscillation. In the case shown in Figure 2-3, the sampling is aligned to each zero-crossing and to the peak values. With any skew from this unique case, there can always be at least 2 samples per half cycle of the sine wave.
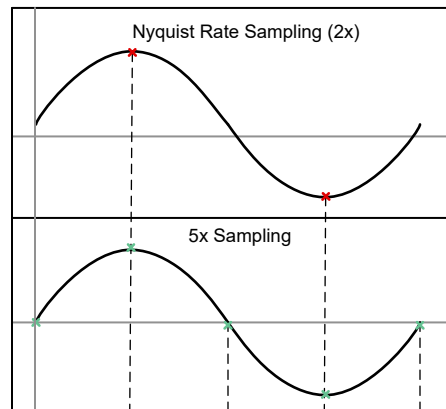
Figure 2-3. Sampling Rates

If 5 samples are used in each 78ms time period, then approximately 15.6ms are available between each sample. To measure cadence with both speed and direction information, using a 3D Hall-effect sensor is helpful. TMAG3001 and TMAG5173-Q1 each are able to sample 2 axes needed for angle sensing in about 75us per sample. Averaging can be enabled to reduce the impact of noise on the end result at the cost of longer integration times. These sensors can average up to 32x per sample, with an effective sample time for two axes near 1.625ms. However, the recommendation in this particular application to not set the averaging higher than is needed. Since the tooth is moving during the duration of the sample period, a high degree of averaging produces unnecessary system delay. Data collected in this report used 8x averaging to limit angle noise.

2.2 Data Collection

For this demonstration, TMAG3001 was used to detect the passage of each tooth. An initial calibration routine is necessary to make full use of the magnetic field to remove the fixed bias produced by the stationary magnet. Figure 2-4 shows the X and Z axis field vector measurements as four teeth of the sprocket rotate near the sensor.
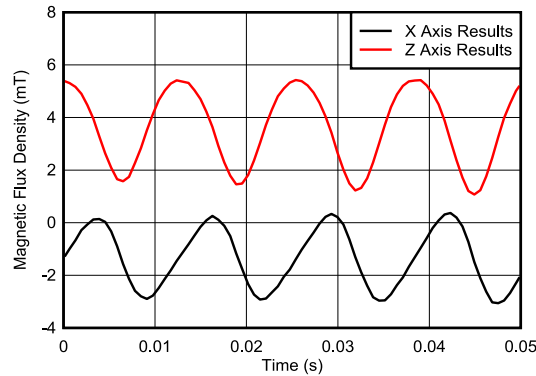
Figure 2-4. Sampled Data

What is seen is that on each axis, an oscillation occurs about some nominal magnetic flux density observed by the Hall-effect sensor. If the pedal crankset were not present, this field can remain static at the back-bias condition. The fixed offset in the measurement presents an immediate challenge to calculations of angle.

The target input for an arctangent angle calculation has X and Y components that follow a cosine and sine behavior with matching amplitude. Plotted as a Lissajous curve in Figure 2-5, this can be easily observed as a unit circle. Similarly plotting the back-biased results in Figure 2-6, significant offset and amplitude mismatch produce an output which can not generate a full 0-360deg angle calculation.
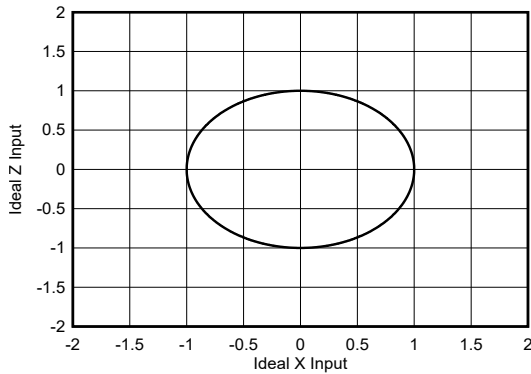
Figure 2-5. Target Output Lissajous Plot
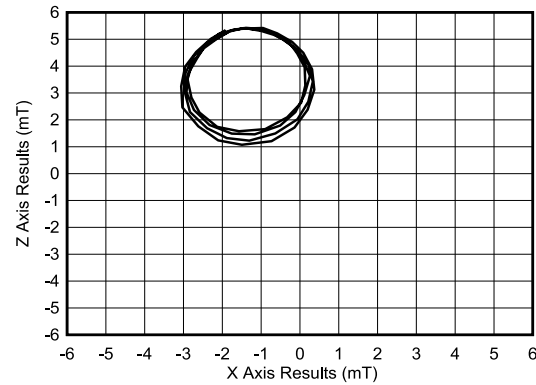
Figure 2-6. Measured Lissajous Plot

Following a brief calibration routine to measure peak output values, the offset to subtract from each measurement can be determined using Equation 1.

$$Offset \ = \ \frac{(Out_{max} + Out_{min})}{2} \tag{1}$$

And the amplitude mismatch can be normalized next by dividing each output by the total amplitude calculated in Equation 2.

$$Amplitude \ = \ (Out_{Max} - \ Out_{Min}) \tag{2}$$

The calibrated result is then found with Equation 3.

$$Calibrated \ Output \ = \ \frac{(Output - Offset)}{Amplitude} \qquad\qquad (3)$$

The resulting shift in the measured data is shown in Figure 2-7 and Figure 2-8.
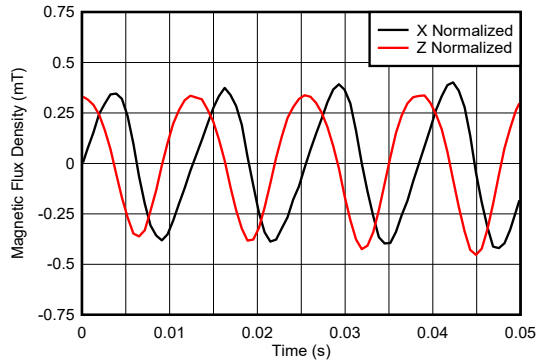
Figure 2-7. Normalized Output Plots
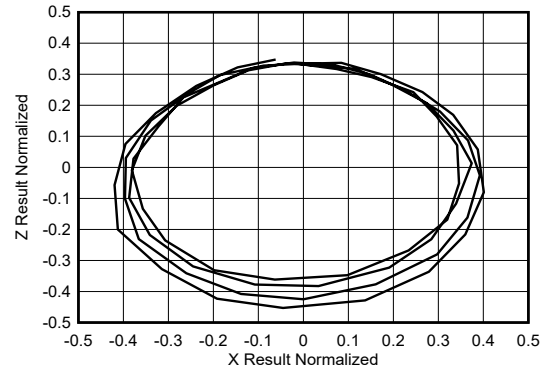
Figure 2-8. Normalized Lissajous Plot

Some skew from tooth to tooth does exist in the output plot, which is related to the chainset sprocket having some tilt relative to the mounting on the bottom bracket axle. This manufacturing defect causes a slight change in proximity to the magnet as the pedals move. For the segment of rotation shown in Figure 2-7 the amplitude was not at the peak value, and so the normalized results do not fully reach ± 0.5mT. Despite this defect, the resulting angle after this brief calibration is shown in Figure 2-9.
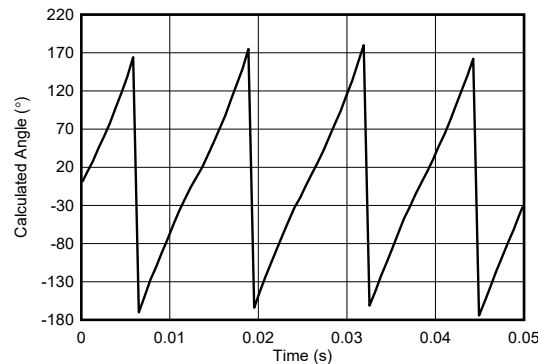
Figure 2-9. Calculated Angle

The resulting calculated angle over the full rotation of the sprocket is shown in relative to the entire gear wheel is shown in Figure 2-10. While some skew is still present to the output angle, the effect of this non-linearity to the overall angle measurement is reduced considering this only represents a small portion of the total rotation. Since the angle output ranges from 0-360 degrees per tooth, the effective angle non-linearity observed on each tooth is divided by the total number of teeth. In this case the number of teeth is 32. Even if an angle non-linearity of 10 degrees were observed for each tooth, the equivalent error can be limited to 0.31 degrees of the entire sprocket rotation.
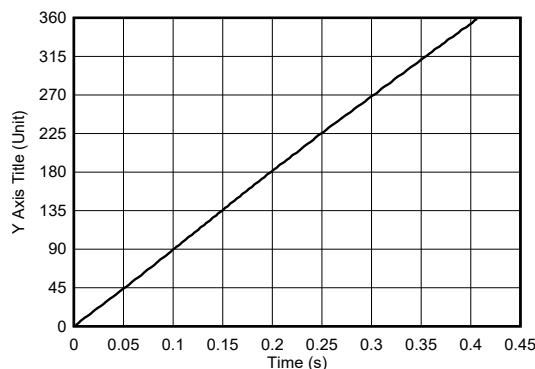
Figure 2-10. Calculated Sprocket Angular Position

The speed of rotation was controlled manually in this demonstration, so some fluctuation in speed was present. To approximate the angle error, the expected change in angle from one sample to the next was determined using the rate of change for the span of one gear tooth. Continuous sampling was used to determine the relative angle change from the start position, and a normalized angle error is shown in Figure 2-11.
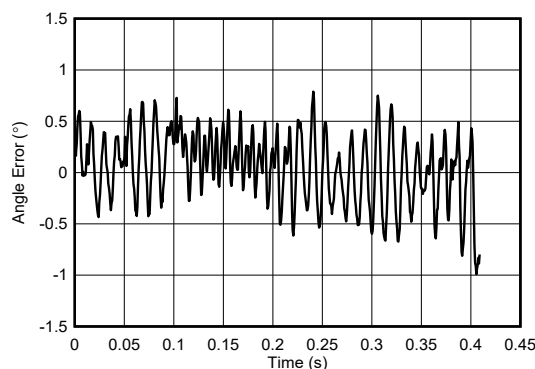
Figure 2-11. Speed Normalized Angle Error

With a 32 tooth gear and a 0-360 degree response per tooth, the resulting relative angle error is less than ±1 mechanical degrees.

2.3 Speed Calculation Methods

There are several approaches to calculating speed using the angle data. Each concept is described in the following sections.

2.3.1 Continuous Sampling

In a continuously sampled configuration, the goal is to measure the rate of change in the measured angle ($\delta\theta/\delta t$) to determine the angular speed of the gear wheel at any given moment. This method can produce a 0-360 degree result for each gear tooth measured and provides direction information as well. This is helpful for systems that need instantaneous feedback.

The drawback with this method is that the sensor must remain active and continuously converting which is less of a designed for battery powered applications. Also, any non-linearities in the angle response can appear to be temporary change in speed which reduces overall system accuracy.

2.3.2 Running Average

Since angle measurements are often able to occur many times per gear tooth, it is also possible to create a running average for $\delta\theta/\delta t$. For a number of samples, n, the system can implement a shift register for the last n results and provide an average value which updates after each sample. While this has the drawback of being a more memory intensive process for the MCU, the calculated speed can update more slowly and predictably. This method is particularly useful in systems that benefit from a gradual change in feedback such as speedometers and human interface controls such as pedal cadence.

2.3.3 Zero-Crossing

In systems that need less resolution, the control loop can be adjusted to look for zero-crossings. Even in cases where there is significant non-linearity, the zero crossing point can occur repeatedly at the same relative point in each gear tooth. Tracking the time between each zero-crossing event can eliminate any concerns with angle linearity that result from the shape of the metal target, but can not accrue extra memory requirements in the MCU.

However, the drawback here is that one full period of travel is required to calculate speed. In the example of a 32 tooth bicycle sprocket, this is 11.25 degrees of rotation. While this is an improvement over the 30deg rotation needed by the 12 magnet degree, the feedback in not as immediate.

2.3.4 Periodic Sampling

A final consideration for sampling patterns is to wake the sensor for a burst of measurements. In cases where the system response remains constant for a longer duration, it can be possible to keep the device in a low power state when not needed to conserve power. At some desired interval, the device can be brought out of low power sleep mode, allowed to calculate $\delta\theta/\delta t$ for n samples, and then return to sleep. This method maintains the benefit of a running average calculation, but only provides periodic updates. Running calculations at wider intervals is desirable to achieve lower power consumption for functions that do not require continuous updates.

3 Summary

The implementation of back-bias magnetic sensing is useful for cases where it is not practical to use several magnets, and contact free sensing is required. This is particularly helpful in applications such as wheel and gear speed detection which is a helpful function that enables anti-lock braking (ABS), speedometers, and other power-train monitoring requirements for both e-bike and automotive systems.

In addition to back-biased magnetic sensing, inductive sense coils can also be designed an implemented with devices such as LDC0851 to track the proximity of rotating conductive surfaces. Application information can be found in the reference materials in Table 4-1.

For more information regarding magnetic sensing in e-bike and automotive applications, please refer to Table 4-1 and Table 4-2.

4 References

Table 4-1. Alternate Device Information

Device	Grade	Temperature Rating	Interface	ASIL Rating	Package Type	Design Considerations
TMAG3001	Commercial	-40C to 125C	I2C: 400kHz, 1000kHz	N/A	WCSP	Featuring a very small chip-scale package size, programmable angle thresholds and selectable I2C addressing
TMAG5173-Q1	Automotive	-40C to 125C	I2C: 400kHz, 1000kHz	ASIL-B	SOT-23	Automotive grade 3D Hall-effect sensor in a small package and I2C communication.
TMAG5170 (TMAG5170-Q1)	Commercial (Automotive)	-40C to 150C	SPI: 10MHz	(ASIL-B)	VSSOP-8	Both automotive and commercial grade devices offer complete magnetic field vector measurements using SPI interface.
TMAG5170D-Q1	Automotive	-40 to 150C	SPI: 10MHz	ASIL-D	TSSOP-16	Independent 3D Hall-effect sensor allow for design into high ASIL-D rated systems
TMAG5273	Commercial	-40C to 125C	I2C: 400kHz,1000kHz	N/A	SOT-23	Low-cost commercial grade device with I2C interface

Table 4-2. Related Content

Title	Content Description
Position Sensing in e-Bike Applications	Summary of functions in e-bikes where position sensors are used
2-Wheeler and 3-Wheeler Traction Drive and reference designs	Links to content related to various functions within an e-bike system connected to the traction inverter
Basic Considerations for Sensors in the Powertrain	White paper discussion of automotive sensing functions within the powertrain.
Inductive Sensing: Switch Applications Made Simple	Introduces inductive sensing applications including gear tooth sensing
LDC Device Selection Guide	Discussion of inductive sensors and help selecting devices

IMPORTANT NOTICE AND DISCLAIMER

TI PROVIDES TECHNICAL AND RELIABILITY DATA (INCLUDING DATA SHEETS), DESIGN RESOURCES (INCLUDING REFERENCE DESIGNS), APPLICATION OR OTHER DESIGN ADVICE, WEB TOOLS, SAFETY INFORMATION, AND OTHER RESOURCES "AS IS" AND WITH ALL FAULTS, AND DISCLAIMS ALL WARRANTIES, EXPRESS AND IMPLIED, INCLUDING WITHOUT LIMITATION ANY IMPLIED WARRANTIES OF MERCHANTABILITY, FITNESS FOR A PARTICULAR PURPOSE OR NON-INFRINGEMENT OF THIRD PARTY INTELLECTUAL PROPERTY RIGHTS.

These resources are intended for skilled developers designing with TI products. You are solely responsible for (1) selecting the appropriate TI products for your application, (2) designing, validating and testing your application, and (3) ensuring your application meets applicable standards, and any other safety, security, regulatory or other requirements.

These resources are subject to change without notice. TI grants you permission to use these resources only for development of an application that uses the TI products described in the resource. Other reproduction and display of these resources is prohibited. No license is granted to any other TI intellectual property right or to any third party intellectual property right. TI disclaims responsibility for, and you will fully indemnify TI and its representatives against, any claims, damages, costs, losses, and liabilities arising out of your use of these resources.

TI's products are provided subject to TI's Terms of Sale or other applicable terms available either on ti.com or provided in conjunction with such TI products. TI's provision of these resources does not expand or otherwise alter TI's applicable warranties or warranty disclaimers for TI products.

TI objects to and rejects any additional or different terms you may have proposed.